

Feasibility of Real-Time Near-Infrared Fluorescence Tracer Imaging in Sentinel Node Biopsy for Oral Cavity Cancer Patients

Anders Christensen, MD^{1,2}, Karina Juhl, MSc², Birgitte Charabi, MD¹, Jann Mortensen, MD, DMSc², Katalin Kiss, MD³, Andreas Kjær, MD, PhD, DMSc², and Christian von Buchwald, MD, DMSc¹

¹Department of Otolaryngology, Head & Neck Surgery and Audiology, Rigshospitalet, Copenhagen University Hospital, Copenhagen, Denmark; ²Department of Clinical Physiology, Nuclear Medicine & PET and Cluster for Molecular Imaging, Rigshospitalet and University of Copenhagen, Copenhagen, Denmark; ³Department of Pathology, Rigshospitalet, Copenhagen University Hospital, Copenhagen, Denmark

ABSTRACT

Background. Sentinel node biopsy (SNB) is an established method in oral squamous cell carcinoma (OSCC) for staging the cN0 neck and to select patients who will benefit from a neck dissection. Near-infrared fluorescence (NIRF) imaging has the potential to improve the SNB procedure by facilitating intraoperative visual identification of the sentinel lymph node (SN). The purpose of this study was to evaluate the feasibility of fluorescence tracer imaging for SN detection in conjunction with conventional radio-guided technique.

Methods. Prospective study of patients with primary OSCC planned for tumor resection and SNB. Thirty patients were injected peritumorally with a bimodal tracer (ICG-^{99m}Tc-Nanocoll) followed by lymphoscintigraphy and SPECT/CT to define the SNs and their anatomical location preoperatively. SNs were detected intraoperatively with a hand-held gamma-probe and a hand-held NIRF camera.

Results. In 29 of 30 subjects (97%), all preoperatively defined SNs could be identified intraoperatively using a combination of radioactive and fluorescence guidance. A total of 94 SNs (mean 3, range 1–5) that were both radioactive and fluorescent ex vivo were harvested. Eleven of 94 SNs (12%) could only be identified in vivo using NIRF imaging, and the majority of those were located in level 1 close to the primary tumor.

Conclusions. A combined fluorescent and radioactive tracer for SNB is feasible, and the additional use of NIRF imaging may improve the accuracy of SN identification in oral cancer patients. Intraoperative fluorescence guidance seems of particular value when SNs are located in close proximity to the injection site.

In head and neck cancer, the presence of metastasis in the tumor draining lymph nodes in the neck is one of the most important prognostic factors for treatment outcome.^{1,2} Sentinel node biopsy (SNB) is gaining acceptance in oral squamous cell carcinoma (OSCC) and has been applied as a standard staging method for the cN0 neck since 2007 in our center.³ Approximately 20–30 % of patients presenting with a cN0 neck harbor subclinical (occult) lymph node metastases and can be identified using SNB, whereas the remaining majority of patients can be spared an unnecessary selective neck dissection and the associated morbidities.^{4,5} A recent meta-analysis of SNB for early OSCC comprising 987 patients showed a sensitivity and negative predictive value of 86 and 94 %, respectively.⁶ The accuracy of conventional radiocolloid-based SNB depends heavily on the ability to correctly identify the true SN intraoperatively guided by a radioactive signal combined with information from preoperative lymphoscintigraphy imaging. Radioactivity is characterized by high tissue penetration but limited spatial resolution, which may affect the accuracy of the intraoperative navigation towards the SN. In particular when the SN is located in close proximity to the injection site where background radioactivity is high, navigation can be difficult or even impossible. In the setting of OSCC, this problem is especially the case for SNs located in level 1 due to complex drainage and close spatial relation to the oral cavity.⁷ A lower

accuracy of the SNB procedure for tumors located in the floor of the mouth (FOM) has been reported in recent larger series, which may be explained by masking of the SN due to radioactive shine-through from the injection site.^{8–10} Near-infrared fluorescence (NIRF)-guided SNB is a novel modality that enables real time intraoperative imaging of the lymphatics within the surgical field with high spatial resolution.^{11,12}

The utility of Indocyanine Green (ICG) for SN mapping has been studied in multiple malignancies suited for the SNB procedure and most comprehensively in breast cancer.^{13–15} Recently, a bimodal approach has been introduced for SNB by exploiting the beneficial hydrodynamic draining properties of radiocolloids and the high affinity of ICG for albumin, thereby assembling a combined tracer complex, which is both fluorescent and radioactive.¹⁶ With a bimodal tracer the preoperative radioactivity-based imaging and surgical planning can be directly combined with the intraoperative detection of the SN with both a visible fluorescent signal and the conventional radioactive (acoustic) signal available for navigation.¹⁷ Accordingly, adding NIRF imaging to the SNB procedure has the potential to improve the accuracy of intraoperative SN detection in OSCC.

The purpose of this study was therefore to evaluate the feasibility of NIRF imaging for SN detection in early oral cancer in conjunction with conventional radioguided technique.

PATIENTS AND METHODS

Between December 2013 and September 2014, 30 patients diagnosed consecutively with primary cN0 T1-T2 OSCC and scheduled for tumor resection and SNB were included in the study. In all the patients, the nodal neck status was evaluated with clinical examination, ultrasound, CT, and/or MRI. Exclusion criteria were prior head and neck cancer, prior surgery or radiotherapy to neck, pregnancy, severe kidney failure, and allergy to ICG or iodine. Patients were enrolled after obtaining informed consent. The first author (AC) assisted in all the operations. The study protocol was conducted in accordance with the Helsinki Declaration and approved by the Danish Regional Scientific Ethical Committee (H-1-2013-091). The study was approved as a single-institution clinical trial by the European Medicines Agency (EudraCT No. 2013-003578-28, www.clinicaltrialsregister.eu) and was monitored and conducted in accordance with GCP standards.

Tracer Preparation and Administration

^{99m}Tc-Nanocoll was prepared by adding 2 GBq of pertechnetate in 2 ml of saline to a vial of Nanocoll

containing 0.5 mg of human albumin colloid (GE Healthcare). The mixture was incubated for 30 min before use. ICG was prepared by adding 5 ml of sterile water to a vial containing 25 mg of dry compound (ICG-Pulsion, Pulsion Medical, Germany) and further diluted to a 0.5 mg/ml of ICG stock solution. Then, 0.1 ml of ^{99m}Tc-Nanocoll (55 or 110 MBq depending on same-day or day-before surgery) and 0.1 ml of ICG stock solution was mixed to a final volume of 0.2 ml of ICG-^{99m}Tc-Nanocoll containing 0.05 mg of ICG (0.32 mM). The tracer was injected submucosally in four peritumoral deposits.

Preoperative Imaging

Lymphoscintigraphy (LSG) and SPECT/CT were performed using a dual head SPECT/CT camera (Precedence SPECT/CT, Philips Healthcare, The Netherlands) in a 60-min scanning protocol. Immediately after tracer injection, a dynamic LSG in anterior and lateral projection was acquired followed by a static LSG 15 min postinjection to identify the temporal order of SN identification. Then, SPECT/CT was performed and images were generated. If the first scanning session did not identify any SN, a second late LSG and SPECT/CT was performed 120 min postinjection. Images were interpreted by a specialist in nuclear medicine, and the localization of the SN was depicted in an anatomical chart of the neck divided into neck levels as proposed by AHNS.¹⁸ The number of SNs detected on LSG and SPECT/CT was recorded. A lymph node clearly visible on LSG or SPECT/CT was considered a SN.

Surgical Procedure and Intraoperative Imaging

Tumor resection and reconstruction was done before the SNB neck procedure. Fluorescence imaging was performed with the clinically approved hand-held NIR camera system and accompanying software (Fluobeam 800, Fluoptics, France). Before skin incision, fluorescence imaging was performed to localize SNs that were visible transcutaneously. During surgery, the NIR camera and a hand-held gamma probe (Neo2000, Neoprobe Corporation, USA) were used in parallel to navigate towards the SN, and the modality (radioactive and/or fluorescent) for identification was recorded. To distinguish a SN from a non-SN, a radioactive count rate less than 10 % of the SN with the highest count rate was applied as a rule. In addition, any lymph node with a bright fluorescent signal was appointed a SN. Intraoperative fluorescence imaging of the SNs in the in situ location was performed before removal, and the exact anatomical location was recorded. The surgical field was searched systematically for any remaining radioactive or fluorescent signal before closure. Operation time for the

SNB in the neck was defined as from skin incision to completed skin closure.

Ex Vivo Imaging and Histology

The harvested SNs were postoperatively imaged with the NIR camera under standardized conditions and aligned beside a reference tube containing a 0.2- μ M ICG solution. Harvested SNs were fixed in formalin for 24 h, paraffin embedded, and processed with step-serial sectioning, using H&E staining and cytokeratin antibodies according to a previously described protocol.⁴ Tumor deposits were classified as macrometastasis, micrometastasis, or isolated tumor cells.¹⁹ Non-SNs encountered during dissection that not could be preserved and therefore resected were examined with routine histopathological analysis. Tissue sections stained with H&E from a selected number of SNs and non-SNs were imaged using a NIR scanner (Odyssey Sa, LI-COR Biosciences, UK).

Data Analysis

For statistical analyses, SAS Enterprise software Version 9.4 was used. A value of $p < 0.05$ was considered statistically significant. Continuous measures were compared using Wilcoxon signed-rank test between groups. On intraoperative and postoperative unsaturated raw grayscale images the fluorescence signal was semiquantified using regions of interest in the software ImageJ (version 1.48, NIH, USA). A Signal-to-Background-Ratio (SBR) and Signal-to-Reference-Ratio (SRR) was calculated by dividing the fluorescent signal of the SN by the fluorescent signal of adjacent tissue intraoperatively or the ICG-reference and standard background postoperatively.

RESULTS

Patient and tumor characteristics are outlined in Table 1. All patients were managed with a transoral tumor resection and a primary closure or a local flap. No adverse reactions or complications related to the hybrid tracer were observed. Six patients (20 %) had a single positive SN and a subsequent selective neck dissection was performed where no additional metastatic deposits were found in the neck specimens on routine histopathology.

Preoperative Imaging

A total of 68 SNs were defined preoperatively and modality for detection is shown in Table 2. In two patients, no SN was detected on the initial imaging and a late second LSG and SPECT/CT was performed where a SN could be

TABLE 1 Patient and tumor characteristics

Characteristic	N or mean	% or range
Age, year (mean, range)		
Men	64	(52–83)
Women	63	(50–79)
Body mass index (mean, range)	24.3	(18.0–32.3)
Tumor subsite location in oral cavity		
Floor of mouth	15	50
Tongue, ant. 2/3	9	30
Inferior tongue	2	7
Buccal	1	3
Hard palate	1	3
Gingiva	1	3
Retromolar trigone	1	3
Tumor crossing midline		
Yes	8	27
No	22	73
Tumor stage		
T1	18	60
T2	12	40
Operation time (min) for SNB neck procedure (mean, range)	39	(15–115)
Pathology		
–SN	88	94
+SN	6	6
Macrometastasis (>2 mm)	3	50
Micrometastasis (≥ 0.2 mm, ≤ 2 mm)	3	50
Isolated tumor cells (<0.2 mm)	0	0
pN staging		
pN0	24	80
pN1	6	20

TABLE 2 Modality for SN identification

Modality for SN identification	N	Detection rate % (n/n)
Preoperatively		
Total no. of SNs visualized	68	71 (68/96)
LSG	41	43 (41/96)
SPECT/CT	68	71 (68/96)
Intraoperatively		
Total no. of SNs harvested	94	98 (94/96)
Fluorescent + radioactive	83	86 (83/96)
Radioactivity only	0	0 (0/96)
Fluorescence only	11	11 (11/96)

detected in both cases. In 18 patients (60 %), bilateral lymphatic drainage was seen, and 1 patient (3 %) with a lateralized FOM tumor had only contralateral drainage.

TABLE 3 Distribution of all harvested SNs stratified by neck side and tumor subsite

Subsite	Ipsilateral neck side by level					Contralateral neck side by level				
	1	2	3	4	5	1	2	3	4	5
FOM	14% (7/50)	42% (21/50)	16% (8/50)	4% (2/50)	2% (1/50)	10% (5/50)	8% (4/50)	4% (2/50)	-	-
Tongue*	6% (2/34)	50% (17/34)	32% (11/34)	3% (1/34)	-	3% (1/34)	-	6% (2/34)	-	-
Other subsites**	50% (5/10)	30% (3/10)	10% (1/10)	-	-	-	10% (1/10)	-	-	-
All subsites	15% (14/94)	43% (40/94)	21% (20/94)	3% (3/94)	1% (1/94)	6% (6/94)	5% (5/94)	4% (4/94)	-	-

FOM tumors showed a higher frequency of lymphatic drainage to both the contralateral level 1 and 2 compared with tongue tumors

FOM floor of mouth

* Anterior 2/3 of tongue and inferior tongue

** Buccal, hard palate, gingiva and retromolar trigone

Intraoperative Imaging and Lymph Node Detection

A total of 94 SNs were detected intraoperatively yielding an average of 3 SNs (range 1–5) per patient; the distribution in the neck is depicted in Table 3. At least one SN was identified in all patients. In one patient with a FOM tumor, two of three preoperatively defined SNs, with an unusual location medial to the mandible within the FOM, could not be located, and the neck procedure was extended to a bilateral neck dissection after which the patient was staged as pN0. Therefore, the intraoperative detection rate of the preoperatively defined SNs was 97 % (66/68). Before skin incision, 10 % (9/94) of the excised SNs could be visualized by fluorescence transcutaneously (Fig. 1). The success of noninvasive transcutaneous SN identification was significantly correlated with a low BMI ($p = 0.05$).

Intraoperatively, 11 SNs in 9 patients could only be identified due to fluorescence. They were all located solitary and not as a part of a cluster of lymph nodes and they were not identified on SPECT/CT (Fig. 2). In seven of nine of the patients, these additional nodes could be detected through the incision made to search level 1 and/or level 2. In two patients with FOM tumors, an additional incision was made in the contralateral neck because transcutaneous NIR imaging demonstrated drainage to level 1, and two additional nodes could be retrieved. These additional SNs were all negative on histology and therefore did not lead to upstaging of patients. No SN was identified only due to the radioactive signal. Ex vivo, all 94 harvested SNs were both radioactive and fluorescent (Table 3). The mean intraoperative SBR of the SNs was 7.8 (range 1.9–30.6). Clusters of 3–5 lymph nodes were often encountered in level 2a where fluorescence enabled easy separation in SNs and non-SNs due to real-time imaging. On micro-fluorescence scanning of tissue slides of SNs and non-SNs anatomically located closely adjacent in a cluster, the fluorescent signal from ICG could be seen distributed within the lymphatic drainage system in the SN while no fluorescent signal could be detected in the non-SN (Fig. 2).

In the 23 patients, who had three or more SNs removed, the fluorescence intensity, measured as SBR or SRR, correlated with the radioactive count both intraoperatively ($p = 0.015$) and ex vivo ($p = 0.007$) when analyzed in a mixed model. Within each patient, a linear correlation between either intraoperative or ex vivo fluorescence intensity and radioactivity was observed (Fig. 3).

DISCUSSION

To our knowledge, this prospective study is the largest to date on fluorescence-guided SNB in OSCC. By adding the fluorescence modality to the SNB procedure, an

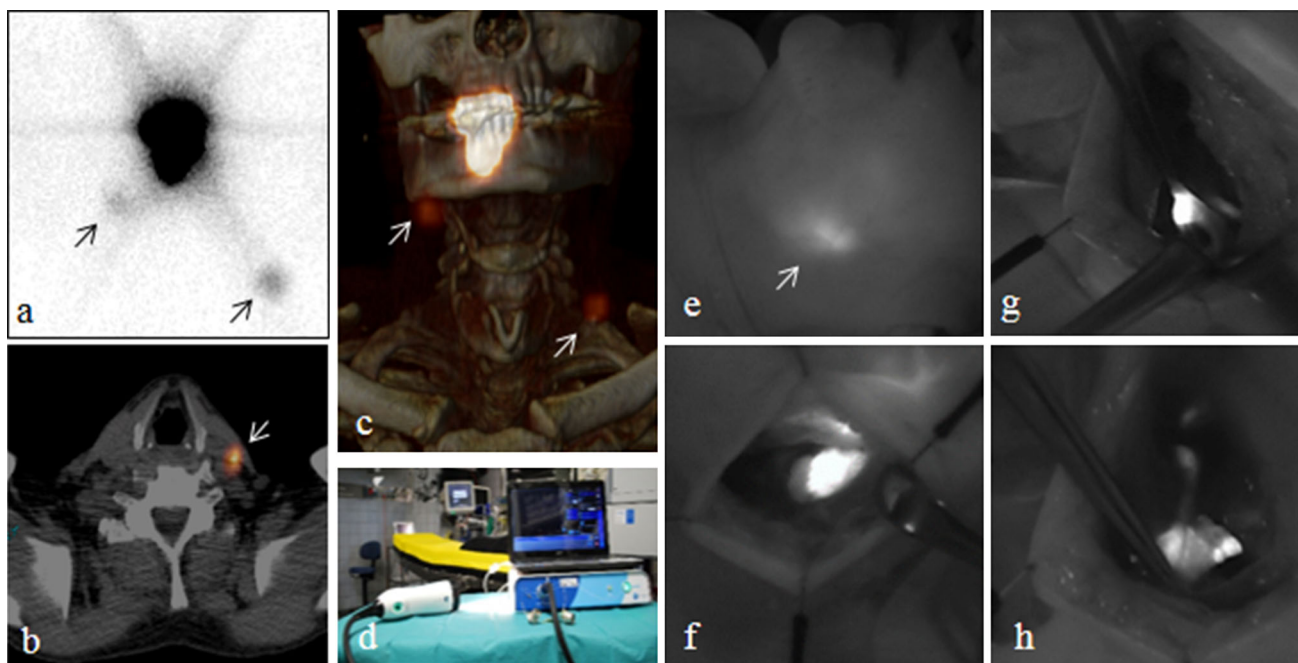


FIG. 1 Preoperative and intraoperative SN imaging. LSG (a), axial SPECT/CT (b), and the 3-D reconstructed SPECT/CT (c) in a patient with a well-lateralized tumor on the right anterior tongue showing tracer drainage to an ipsilateral SN in level 1 and directly to a contralateral SN in level 3 (arrows). The latter SN in level 3 in the left neck side was visible transcutaneously (e). The Fluobeam 800 NIR camera (d) designed for ICG imaging. The NIR camera entered the surgical field in a sterile cover, and real-time video imaging was

presented for the surgical team on a clinical screen. When using the NIR camera intraoperatively, the direct surgical light was turned off to improve the quality of the imaging. The system has a 750-nm excitation laser and LED white light illumination of the surgical field that does not inflict on the NIRF imaging. The hand-held camera head is maneuverable in all angles and has a $\times 10$ zoom function. The autofocus function allows for flexible working distance. Intraoperative NIRF-guided identification and resection of SN (f, g, h)

additional 11 SNs were detected that otherwise would have been left behind when using conventional radioguided technique. Anatomically, the additional SNs were located almost exclusively in level 1 close to the injection site in the oral cavity and, therefore, demonstrate that intraoperative fluorescence imaging enables navigation towards SNs otherwise masked by the radioactive background signal. These findings support a recent similar study of SN detection in 14 N0 OSCC patients using ICG- ^{99m}Tc -Nanocoll.²⁰ In addition, an added value of the SNB hybrid tracer principle for melanoma in the head and neck region has been reported.²¹

We found SPECT/CT superior to LSG in terms of preoperative SN detection, which previously has been reported by our group and others.^{22,23} In addition, SPECT/CT provided very accurate anatomical information about SN location useful for planning of surgery, and we recommend SPECT/CT to be an integrated part of SNB procedures in the head and neck region.

The yield of subclinical metastases was 20 %, which is low compared with other series that reflect that 60 % were T1 tumors with a lower risk of metastatic spread compared with higher T-stage tumors. We observed a high percentage

(60 %) of bilateral drainage probably, because the majority of the tumors in this cohort was in the FOM.

We observed an excellent retention of ICG- ^{99m}Tc -Nanocoll in the SN, even in patients injected the day before the SNB procedure, while drainage to second tier nodes downstream was minimal. This probably reflects that the hybrid tracer has the beneficial hydrodynamic characteristics of Nanocoll for SN mapping.²⁴ In addition, the strong correlation between fluorescence intensity and radioactivity in the SNs within each patient in our study indicates that the hybrid tracer complex remains stable in vivo. This is in accordance with results reported by van der Poel et al. in prostate cancer patients.²⁵ For future studies, this observation also has the implication that only nodes that are both fluorescent and radioactive after resection should be regarded as true SNs.

NIRF-guided SNB mapping using unmixed ICG in oral and oropharyngeal cancer has been reported in a few studies where problems with rapid transportation of ICG to higher echelon nodes were noted.^{26,27} When performing NIRF-guided SNB in head and neck cancer patients, strong tracer retention in the SN and minimal overflow to higher echelon nodes is of paramount importance, which depends

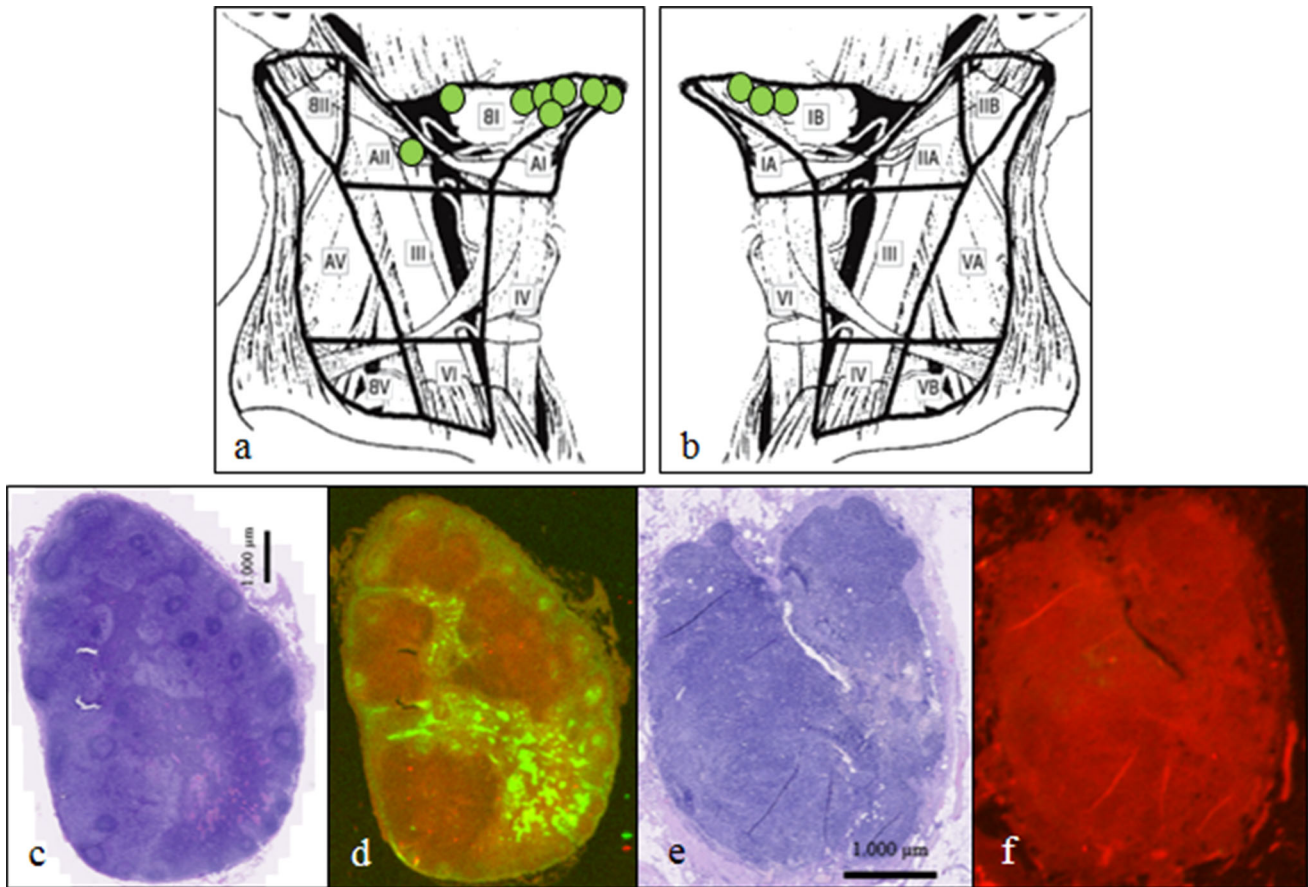
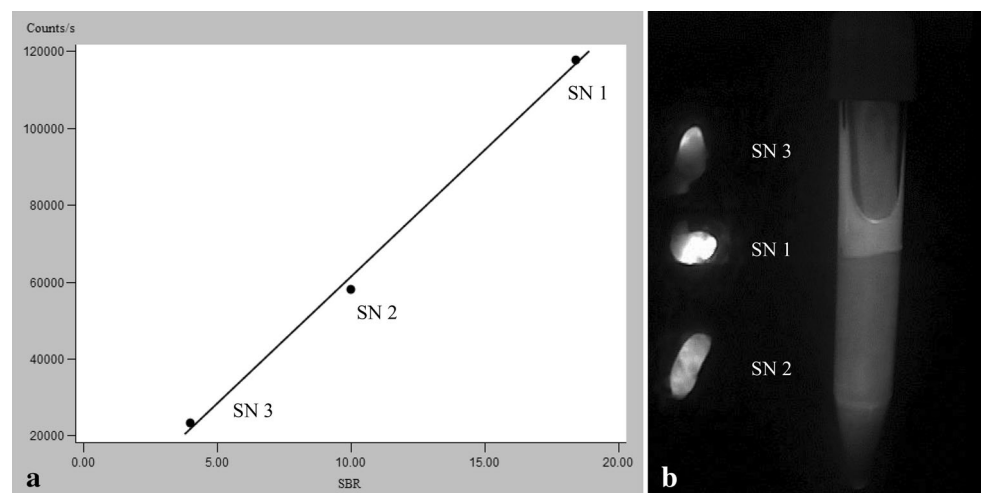


FIG. 2 Intraoperative SN identification by NIRF imaging only. The exact anatomical location and neck level location in the ipsilateral (a) and contralateral (b) neck side of the 11 additional SNs identified only by fluorescence. H&E staining and fluorescence microimaging of a tissue section from a SN (c and d) and a non-SN (e and f) located

intimately within the same cluster of lymph nodes in level 2a. None of the lymph nodes contains metastatic tumor. In the SN the microanatomical distribution of the fluorescent tracer draining from the marginal sinus towards the medullary sinus is visualized. The non-SN is without any signal from ICG on NIRF microimaging

FIG. 3 Correlation between the fluorescent and the radioactive signal. A representative case example (a) of linear correlation between the intraoperative fluorescent and the radioactive signal in three resected SNs from the same patient. Postoperative NIRF imaging (b) of the same three SNs aligned besides a reference tube containing a 0.2- μ M ICG concentration



on the use of a carrier colloid. In breast cancer, the use of unmixed ICG, which has a hydrodynamic diameter <1 nm, has proven to be successful, because direct transcutaneous dynamic visualization of the rapid tracer flow towards the

SN within minutes is possible.²⁸ However, this is not the case in the neck, and in our opinion initial radioguidance is still required for lymphatic SN mapping in head and neck cancer.

Similar to results by Crane et al. using unmixed ICG for SNB in vulvar cancer, we found the transcutaneous fluorescence signal to be correlated to the BMI of the patient and that transcutaneous node mapping was not feasible.²⁹ The fluorescent signal from ICG has a limited tissue penetration of approximately 0.5–1.5 cm. Accordingly, in our study some exploration in the surgical field was necessary in the majority of cases to obtain successful NIRF imaging of the SN.

Clusters of closely located lymph nodes embedded in fatty tissue in the neck are common, and in the present study NIRF imaging enabled direct visual differentiation of SN from non-SNs for selective dissection of the SN. In addition, often only one of several lymph nodes within a cluster was the tumor draining SN. This supports the SNB theory of timely ordered and individual lymph node drainage patterns. By the NIRF imaging approach, the risk of sending non-SNs for expensive thorough SN pathology examination may be limited.

To prove an added value of NIRF-guided SNB in head and neck cancer, future studies with follow-up data of N-site recurrences in SN-negative patients are needed to address the false-negative rate stratified for tumor subsites.

In conclusion, a combined fluorescent and radioactive tracer approach for SNB is feasible and additional use of NIRF imaging may improve the accuracy of SN identification in OSCC. Intraoperative fluorescence guidance seems of particular value when SNs are located in close proximity to the injection site.

ACKNOWLEDGMENT The authors thank the head and neck surgeons, Christoffer Holst Hahn, Janne Rasmussen, Christel Lajer, Thomas Frisch, Jesper Tvedskov, and Irene Wessel, The Head and Neck Division in the Department of Otolaryngology, Head & Neck Surgery for their contribution. A special thanks to Mette Møller Jørgensen and Tim Lundby for technical support in the Department of Clinical Physiology, Nuclear Medicine & PET. This work was supported by the University of Copenhagen, Toyota Fonden, Agnes og Poul Friis Fond, and Harboefonden.

DISCLOSURES The authors declare that they have no financial or other conflicts of interest regarding material discussed in this manuscript. GE Healthcare supported the study with Nanocoll as product free of charge and had no influence on the preparation or conduction of the study.

OPEN ACCESS This article is distributed under the terms of the Creative Commons Attribution 4.0 International License (<http://creativecommons.org/licenses/by/4.0/>), which permits unrestricted use, distribution, and reproduction in any medium, provided you give appropriate credit to the original author(s) and the source, provide a link to the Creative Commons license, and indicate if changes were made.

REFERENCES

- Layland MK, Sessions DG, Lenox J. The influence of lymph node metastasis in the treatment of squamous cell carcinoma of the oral cavity, oropharynx, larynx, and hypopharynx: N0 versus N+. *Laryngoscope*. 2005;115(4):629–39.
- Tankere F, Camproux A, Barry B, Guedon C, Depondt J, Gehanno P. Prognostic value of lymph node involvement in oral cancers: a study of 137 cases. *Laryngoscope*. 2000;110(12):2061–5.
- Pedersen NJ, Hebbelstrup JD, Hedback N, et al. Staging of early lymph node metastases with the sentinel lymph node technique and predictive factors in T1/T2 oral cavity cancer: a retrospective single-center study of 253 consecutive patients. *Head Neck*. 2015.
- Christensen A, Bilde A, Therkildsen MH, et al. The prevalence of occult metastases in nonsentinel lymph nodes after step-serial sectioning and immunohistochemistry in cN0 oral squamous cell carcinoma. *Laryngoscope*. 2011;121(2):294–8.
- Bilde A, von Buchwald C, Therkildsen MH, et al. Need for intensive histopathologic analysis to determine lymph node metastases when using sentinel node biopsy in oral cancer. *Laryngoscope*. 2008;118(3):408–14.
- Yamauchi K, Kogashiwa Y, Nakamura T, Moro Y, Nagafuji H, Kohno N. Diagnostic evaluation of sentinel lymph node biopsy in early head and neck squamous cell carcinoma: a meta-analysis. *Head Neck*. 2015;37(1):127–33.
- Alkureishi LW, Burak Z, Alvarez JA, et al. Joint practice guidelines for radionuclide lymphoscintigraphy for sentinel node localization in oral/oropharyngeal squamous cell carcinoma. *Ann Surg Oncol*. 2009;16(11):3190–210.
- Civantos FJ, Zitsch RP, Schuller DE, et al. Sentinel lymph node biopsy accurately stages the regional lymph nodes for T1–T2 oral squamous cell carcinomas: results of a prospective multi-institutional trial. *J Clin Oncol*. 2010;28(8):1395–400.
- Alkureishi LW, Ross GL, Shoaib T, et al. Sentinel node biopsy in head and neck squamous cell cancer: 5-year follow-up of a European multicenter trial. *Ann Surg Oncol*. 2010;17(9):2459–64.
- Hornstra MT, Alkureishi LW, Ross GL, Shoaib T, Soutar DS. Predictive factors for failure to identify sentinel nodes in head and neck squamous cell carcinoma. *Head Neck*. 2008;30(7):858–62.
- Gioux S, Choi HS, Frangioni JV. Image-guided surgery using invisible near-infrared light: fundamentals of clinical translation. *Mol Imaging*. 2010;9(5):237–55.
- Vahrmeijer AL, Hutteman M, van der Vorst JR, van de Velde CJ, Frangioni JV. Image-guided cancer surgery using near-infrared fluorescence. *Nat Rev Clin Oncol*. 2013;10(9):507–18.
- Marshall MV, Rasmussen JC, Tan IC, et al. Near-infrared fluorescence imaging in humans with indocyanine green: a review and update. *Open Surg Oncol J*. 2010;2(2):12–25.
- Verbeek FP, Troyan SL, Mieog JS, et al. Near-infrared fluorescence sentinel lymph node mapping in breast cancer: a multicenter experience. *Breast Cancer Res Treat*. 2014;143(2):333–42.
- Xiong L, Gazyakan E, Yang W, et al. Indocyanine green fluorescence-guided sentinel node biopsy: a meta-analysis on detection rate and diagnostic performance. *Eur J Surg Oncol*. 2014;40(7):843–9.
- Buckle T, van Leeuwen AC, Chin PT, et al. A self-assembled multimodal complex for combined pre- and intraoperative imaging of the sentinel lymph node. *Nanotechnology*. 2010;21(35):355101.
- Brouwer OR, Buckle T, Vermeeren L, et al. Comparing the hybrid fluorescent-radioactive tracer indocyanine green-99mTc-nanocolloid with 99mTc-nanocolloid for sentinel node identification: a validation study using lymphoscintigraphy and SPECT/CT. *J Nucl Med*. 2012;53(7):1034–40.
- Robbins KT, Shaha AR, Medina JE, et al. Consensus statement on the classification and terminology of neck dissection. *Arch Otolaryngol Head Neck Surg*. 2008;134(5):536–8.
- Hermanek P, Hutter RV, Sobin LH, Wittekind C. International Union against cancer. Classification of isolated tumor cells and micrometastasis. *Cancer*. 1999;86(12):2668–73.

20. van den Berg NS, Brouwer OR, Klop WM, et al. Concomitant radio- and fluorescence-guided sentinel lymph node biopsy in squamous cell carcinoma of the oral cavity using ICG-(99m)Tc-nanocolloid. *Eur J Nucl Med Mol Imaging*. 2012;39(7):1128–36.
21. Frontado LM, Brouwer OR, van den Berg NS, et al. Added value of the hybrid tracer indocyanine green-99mTc-nanocolloid for sentinel node biopsy in a series of patients with different lymphatic drainage patterns. *Rev Esp Med Nucl Imagen Mol*. 2013;32(4):227–33.
22. Bilde A, von Buchwald C, Mortensen J, et al. The role of SPECT-CT in the lymphoscintigraphic identification of sentinel nodes in patients with oral cancer. *Acta Otolaryngol*. 2006;126(10):1096–103.
23. Khafif A, Schneebaum S, Fliss DM, et al. Lymphoscintigraphy for sentinel node mapping using a hybrid single photon emission CT (SPECT)/CT system in oral cavity squamous cell carcinoma. *Head Neck*. 2006;28(10):874–9.
24. van Leeuwen AC, Buckle T, Bendle G, et al. Tracer-cocktail injections for combined pre- and intraoperative multimodal imaging of lymph nodes in a spontaneous mouse prostate tumor model. *J Biomed Opt*. 2011;16(1):016004.
25. van der Poel HG, Buckle T, Brouwer OR, Valdes Olmos RA, van Leeuwen FW. Intraoperative laparoscopic fluorescence guidance to the sentinel lymph node in prostate cancer patients: clinical proof of concept of an integrated functional imaging approach using a multimodal tracer. *Eur Urol*. 2011;60(4):826–33.
26. Bredell MG. Sentinel lymph node mapping by indocyanin green fluorescence imaging in oropharyngeal cancer: preliminary experience. *Head Neck Oncol*. 2010;2:31.
27. Nakamura T, Kogashiwa Y, Nagafuji H, Yamauchi K, Kohno N. Validity of sentinel lymph node biopsy by ICG fluorescence for early head and neck cancer. *Anticancer Res*. 2015;35(3):1669–74.
28. Hirche C, Mohr Z, Kneif S, Murawa D, Hunerbein M. High rate of solitary sentinel node metastases identification by fluorescence-guided lymphatic imaging in breast cancer. *J Surg Oncol*. 2012;105(2):162–6.
29. Crane LM, Themelis G, Arts HJ, et al. Intraoperative near-infrared fluorescence imaging for sentinel lymph node detection in vulvar cancer: first clinical results. *Gynecol Oncol*. 2011;120(2):291–5.